Ecology, 96(4), 2015, pp. 972–985

Linking environmental filtering and disequilibrium to biogeography with a community climate framework

Benjamin Blonder,[1,2,14] David Nogués-Bravo,[1] Michael K. Borregaard,[3] John C. Donoghue II,[1,4] Peter M. Jørgensen,[5] Nathan J. B. Kraft,[6] Jean-Philippe Lessard,[7,12] Naia Morueta-Holme,[8] Brody Sandel,[8] Jens-Christian Svenning,[8] Cyrille Violle,[9] Carsten Rahbek,[1,10] and Brian J. Enquist [2,11,13]

[1]*Center for Macroecology, Evolution, and Climate, Natural History Museum of Denmark, University of Copenhagen, Copenhagen 2100 Denmark*
[2]*Department of Ecology and Evolutionary Biology, University of Arizona, Tucson, Arizona 85721 USA*
[3]*School of Geography and the Environment, University of Oxford, Oxford OX1 2JD United Kingdom*
[4]*Center for Conservation Biology, University of California, Riverside, California 92521 USA*
[5]*Missouri Botanical Garden, St. Louis, Missouri 63110 USA*
[6]*Department of Biology, University of Maryland, College Park, Maryland 20742 USA*
[7]*Quebec Centre for Biodiversity Science, Department of Biology, McGill University, Montreal, Quebec H3A 0G4 Canada*
[8]*Section for Ecoinformatics & Biodiversity, Department of Bioscience, Aarhus University, Aarhus 8000 Denmark*
[9]*Centre d'Ecologie Fonctionnelle et Evolutive, Centre National de la Recherche Scientifique, Montpellier 34293 France*
[10]*Imperial College London, Silwood Park, Buckhurst Road, Ascot, Berkshire SL5 7PY United Kingdom*
[11]*Santa Fe Institute, Santa Fe, New Mexico 87501 USA*
[12]*Department of Biology, Concordia University, Montreal, Quebec H4B-1R6 Canada*
[13]*Aspen Center for Environmental Studies, 100 Puppy Smith Street, Aspen, Colorado 81611 USA*

Abstract. We present a framework to measure the strength of environmental filtering and disequilibrium of the species composition of a local community across time, relative to past, current, and future climates. We demonstrate the framework by measuring the impact of climate change on New World forests, integrating data for climate niches of more than 14 000 species, community composition of 471 New World forest plots, and observed climate across the most recent glacial–interglacial interval. We show that a majority of communities have species compositions that are strongly filtered and are more in equilibrium with current climate than random samples from the regional pool. Variation in the level of current community disequilibrium can be predicted from Last Glacial Maximum climate and will increase with near-future climate change.

Key words: climate change; climate mismatch; community assembly; community structure; disequilibrium; environmental filtering; fundamental niche; lag; New World forests; regional species pool.

Introduction

A major challenge in ecology is understanding and predicting the response of communities to changing climates, past, present, and future. A key issue is that species' responses may not be instantaneous or optimal. As a result, local community composition may not accurately reflect shifting abiotic conditions (Svenning and Sandel 2013). We propose that novel insights into how communities respond to environmental change can be found by reframing community structure directly in terms of patterns and processes linked to climate niches. Specifically, we focus on the influence of environmental filtering and environmental disequilibrium. We define environmental filtering as a process creating communities composed of species with more similar climate niches relative to the species in the regional pool and environmental disequilibrium as a pattern indicating communities composed of species with climate niches less close to the local observed climate relative to the species in the regional pool. Community structure may therefore be understood as the outcome of interactions between environmental filtering and disequilibrium.

There is empirical evidence for both environmental filtering and environmental disequilibrium in real communities. Filtering can occur in extreme environments that reduce viable strategies for plants at high elevations (Pottier et al. 2012) and high latitudes (Swenson and Enquist 2007, Hawkins et al. 2013). Disequilibrium can occur when bird species do not fully track contemporary change in winter minimum temperature (La Sorte and Jetz 2012) or when plants (Bertrand et al. 2011, Ordonez 2013, Svenning and Sandel 2013) and butterflies (Devictor et al. 2012) lag in their response to climate change. Better understandings of communities' disequilibrium dynamics are needed for predicting and managing community response to near-future global change.

We develop a framework that can improve inference of climate effects on communities, based on analyzing

Manuscript received 28 March 2014; revised 12 September 2014; accepted 17 September 2014. Corresponding Editor: L. S. Adler.
[14] E-mail: bblonder@gmail.com

TABLE 1. Summary of interpretation of community climate statistics.

Metric	Name	Interpretation	Smaller values mean	Larger values mean
$\Delta_C(t_{\text{inf}})$	community climate volume	climate niche volume occupied by species in community at time t_{inf}	more specialist species or species from fewer biogeographic regions	more generalist species or species from more biogeographic regions
$\delta_C(t_{\text{inf}})$	community climate volume deviation	climate niche volume occupied by species in community at time t_{inf}, relative to niche volume for species in a random sample from regional species pool	<0: environmental filtering	>0: environmental permissiveness or unmeasured microclimate variation
$\lvert\vec{\Lambda}_C(t_{inf}, t_{\text{obs}})\rvert$	community climate mismatch	distance between inferred climate at time t_{inf} from observed climate at t_{obs}	community near climatic center of biogeographic region	community near edge of biogeographic region
$\lambda_C(t_{\text{inf}},t_{\text{obs}})$	community climate mismatch deviation	distance between inferred climate at time t_{inf} from observed climate at t_{obs}, relative to distance for species from a random sample from regional species pool	<0: environmental equilibrium	>0: environmental disequilibrium

community composition, observed climate, and species' climate niches. Our approach aims to detect the signal of environmental filtering and environmental disequilibrium in communities over time. We show how to quantify environmental filtering and disequilibrium using community climate statistics and demonstrate the framework with an analysis of New World forest communities, investigating the signals of environmental filtering and disequilibrium relative to past, present, and future climates.

COMMUNITY CLIMATE FRAMEWORK

Our framework is useful for measuring community structure in two contexts: unscaled (whether the strength of filtering and mismatch is large) and scaled (whether the strength differs in the local community relative to the regional species pool). The unscaled approach is useful for comparing the structures of communities and delineating species pools. The scaled approach is useful for assessing local community assembly processes. Thus, both approaches provide complementary information. Moreover, the scaled approach complements phylogenetic (Webb et al. 2002) and trait-based (Kraft et al. 2008) frameworks for understanding community structure by generating inferences from complementary climate-niche data.

Our framework integrates information on species' broadscale climate niches, the species composition of the local community, the surrounding region, and local climate conditions. These data are combined via a community climate diagram, from which we derive two statistics (Table 1). These statistics are calculated for the climate inferred from community composition at time t_{inf} relative to the observed climate at time t_{obs} and are analyzed alone (unscaled) or after controlling for differences in regional pool composition (scaled).

We provide an illustrated description of the approach in Fig. 1, as well as a complete mathematical formulation in the *Materials and methods*. Our community climate framework is implemented as an R package (comclim; R Development Core Team 2007) and can easily be applied to other data sets.

Definitions and data

Consider a regional pool of species, P, at time t_{inf}. For each species i, we first infer each species' realized climate niche at time t_{inf}, $N_i(t_{\text{inf}})$, in n-dimensional environmental space by transforming geographic observations using a set of climate layers (Fig. 1A). We next consider a community C, whose composition is a subset of P, at time t_{inf}. Suppose also that the observed climate at C at time t_{obs} is $\vec{E}_{\text{obs}}(t_{\text{obs}})$, as measured by weather stations, calculated by general circulation models, or determined from proxies. We then define the inferred climate of the community at t_{inf}, $\vec{E}_{\text{inf}}(t_{\text{inf}})$. The inferred climate is the point in climate space that is the center of all species' realized niches, giving equal weight to all species (Eq. 1). This concept is similar to a multidimensional version of an Ellenberg indicator value (Lenoir et al. 2013), a community inferred temperature (Devictor et al. 2012), or a transfer-function or coexistence-interval climate reconstruction (Birks 1998, Mosbrugger et al. 2005).

The observed climate and species composition of a community can be visualized together on a community climate diagram (Fig. 1B). This diagram is drawn in n-dimensional climate space and is visualized as bivariate plots for each combination of variable pairs. First, the climate niches for all species that occur in the community are drawn as a dot for each species' niche centroid. Second, the observed climate of the community at time t_{obs} is drawn as a black circle. More than one black circle can be used to represent the local climatic conditions at multiple points in time (e.g., as in Fig. 2). Third, the inferred climate at t_{inf} is drawn as a black circle.

A community climate diagram is summarized by two statistics: community climate volume and community climate mismatch. The climate volume is related to environmental filtering and measures the total amount of climate space occupied by overlapping all species in

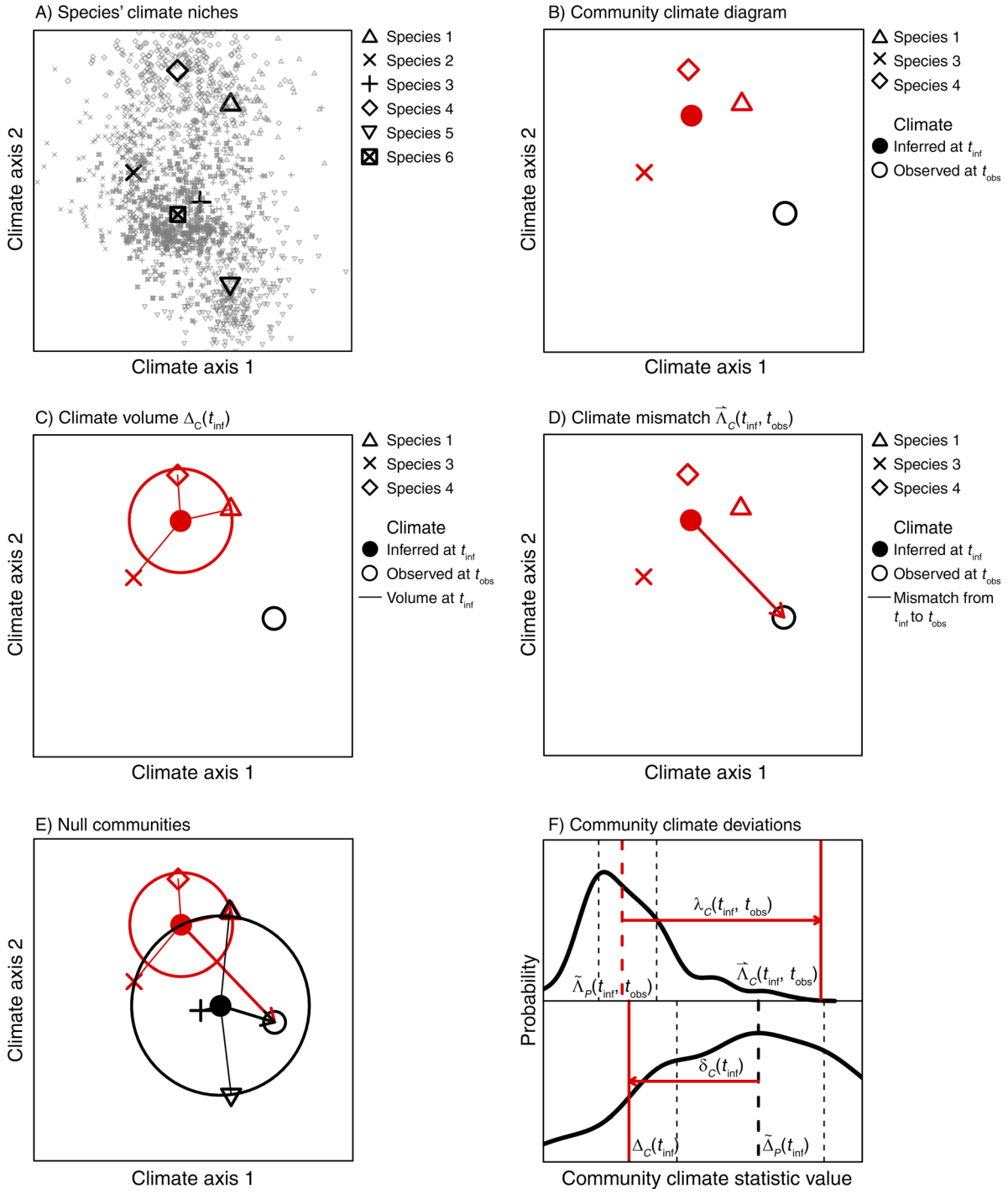

FIG. 1. Summary of our community climate framework. (A) Climate niches for six species in a regional pool are determined from observations (gray symbols; centroid as black symbols). (B) A community climate diagram showing local species composition at time t_{inf} (centroids in red symbols) and observed climate (black circle) at time t_{obs}. The inferred climate (black dot) indicates the climate point in the middle of all species' occurrences at t_{inf}. (C) Community climate volume $\Delta_C(t_{inf})$ indicates the climate space occupied by species in the community at t_{inf}, accounting for the niche breadth of each species. It is drawn as a red circle with radius proportional to the calculated volume. (D) Community climate mismatch $\vec{\Lambda}_C(t_{inf}, t_{obs})$ from t_{inf} to t_{obs} is the vector between inferred climate at t_{inf} and observed climate at t_{obs} and indicates mismatch between species composition and climate. It is drawn as a red arrow with length and direction equivalent to the mismatch vector. In (E), a null distribution of these statistics (black) is generated by sampling random communities from the regional pool, and in (F), community climate deviations ($\delta_C(t_{inf})$ and $\lambda_C(t_{inf}, t_{obs})$; red arrows) are computed by comparing the observed statistics (red vertical line) to the null distributions (black curves; vertical short-dashed gray lines are 25% and 75% quartiles, and the vertical long-dashed black line is the median).

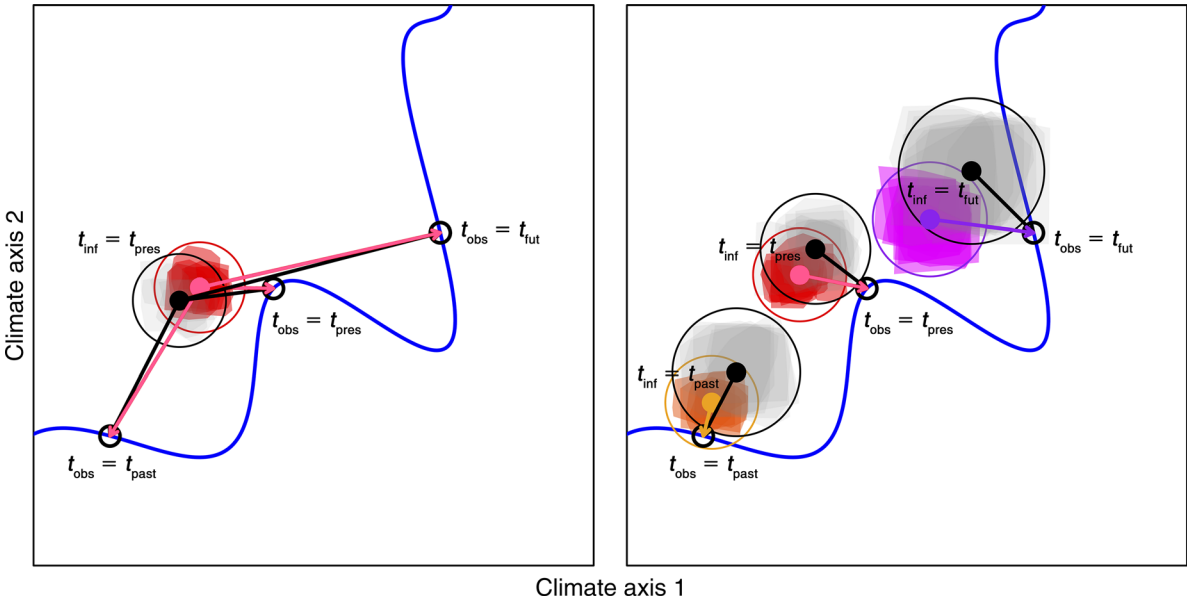

FIG. 2. Two ways to use our community climate framework across time. Consider a single community at different times, t_{inf} and t_{obs}. The community's composition at any time t_{inf} is shown as colored climate envelopes and centroids (null expectations in gray), while the trajectory of the observed climate over times t_{obs} is shown as a blue line. (A) Lag times for community assembly can be determined. If the community composition is known at one time t_{inf} and the observed climate is known at multiple times t_{obs}, then a single value of $\delta_C(t_{inf})$ but multiple values of $\lambda_C(t_{inf},t_{obs})$ can be calculated. The time t_{obs}, for which $\lambda_C(t_{inf},t_{obs})$ is minimized, indicates when the community's composition at t_{inf} was determined by environmental filtering. (B) Temporal variation in assembly processes can be inferred. If the community composition, climate niches, and the observed climate are known at multiple times, and the investigator sets $t_{inf} = t_{obs}$, then multiple values of both $\delta_C(t_{inf})$ and $\lambda_C(t_{inf},t_{obs})$ can be calculated. The resulting time series reflect the strength of environmental filtering and disequilibrium over time.

the community (Fig. 1C), taking into account their niche breadths. We define community climate volume, $\Delta_C(t_{inf})$, via a one-dimensional proxy, as the mean median distance between the inferred climate and random samples from all species' niches in the community (Eq. 2). The climate mismatch is related to disequilibrium and measures the distance between the community's inferred climate at one time and the observed climate at the same or another time (Fig. 1D). We define the community climate mismatch, $\vec{\Lambda}_C(t_{inf}, t_{obs})$ as the vector between the inferred climate at time t_{inf} and the observed climate at time t_{obs} (Eq. 3). Note that this mismatch is between the mean community inferred climate and the observed climate. Hence, a nonzero mismatch may not mean that the observed climate is outside what the species in the community can tolerate, if the component species have sufficient niche breadth (i.e., limited filtering, such that $\Delta_C(t_{inf}) \geq |\vec{\Lambda}_C(t_{inf}, t_{obs})|$).

It is important to note that because these statistics use a Euclidean distance metric, the magnitudes of climate axes must be comparable. As a result, all climate axes should be rescaled (e.g., by logarithmic or z-score transformation) prior to analysis.

Unscaled analysis of community climate statistics

Raw values of these statistics can provide novel insights into comparative biogeography. For example, a community with a large value of $\Delta_C(t_{inf})$ (relative to other communities) has a composition that includes species with broader and/or more distinct climate niches at t_{inf}. Such a pattern may reflect a community populated by generalists or by a mixture of species from several biogeographic regions. A small value of $\Delta_C(t_{inf})$ may reflect more specialist species or species from fewer biogeographic regions. A community with a large value of $|\vec{\Lambda}_C(t_{inf}, t_{obs})|$ has a composition at t_{inf}, including species whose niche centroids are far away from the observed climate at t_{obs}. Such a pattern may reflect a community located at or beyond the margin of most species' climate niches, i.e., at the interface of biogeographic regions. A small value of $|\vec{\Lambda}_C(t_{inf}, t_{obs})|$ may instead reflect a community located in the center of most species' climate niches. These statistics can be compared across communities through a regression approach in which multiple communities' statistics are plotted as a function of another predictor variable, e.g., latitude, as in Fig. 4.

Scaled analysis of community climate deviations

Scaled values of community climate statistics can provide insights into local community assembly from the biogeographic processes that may influence unscaled values of community climate statistics. By comparing community climate statistics from their null expectation (Fig. 1E), we can infer the strength of filtering and

disequilibrium in the local community relative to the regional expectation.

We draw a random sample of species from the regional pool P at t_{inf} with richness equal to that of the community at t_{inf}. Lessard et al. (2012*b*) provide guidelines on choosing an appropriate regional pool. Different research questions can be addressed depending on the scale chosen for the local community and the regional pool. For example, one could ask questions of filtering of species into a 0.1-ha plot (local community 1) relative to species on a 50-ha island (regional pool 1), or alternatively, questions of disequilibrium into an aquatic microcosm (local community 2) relative to a single lake (regional pool 2) or a set of lakes (regional pool 3). Community climate deviations therefore describe a property of a local community relative to the chosen regional pool. However, the framework does not distinguish processes determining the species composition of the regional pool itself. A useful analogy is a person walking backward (local community 3) on a train that is moving forward (regional pool 4). The person is in disequilibrium with the train (regional pool 4), but could simultaneously be in equilibrium with the ground (regional pool 5). Thus the inference depends on the reference point in the analogy and in the framework.

We calculate community climate statistics for this null community sampled from the regional pool, $\Delta_P(t_{\text{inf}})$ and $\vec{\Lambda}_P(t_{\text{inf}}, t_{\text{obs}})$, and repeat this sampling process a large number of times to generate null regional distributions, $\tilde{\Delta}_P(t_{\text{inf}})$and $\tilde{\Lambda}_P(t_{\text{inf}}, t_{\text{obs}})$. We then calculate community climate deviations using a function, $\Omega(A_{\text{obs}},A_{\text{null}})$, that computes a standardized effect size for an observed statistic, A_{obs}, by its null distribution, A_{null} (Eq. 4). Significance of each deviation can be determined from P values based on resampling methods (Eq. 5). We define community climate volume deviation as

$$\delta_C(t_{\text{inf}}) = \Omega(\Delta_C(t_{\text{inf}}), \tilde{\Delta}_P(t_{\text{inf}})) \quad (1)$$

and community climate mismatch deviation as

$$\lambda_C(t_{\text{inf}}, t_{\text{obs}}) = \Omega\Big(|\vec{\Lambda}_C(t_{\text{inf}}, t_{\text{obs}})|, |\tilde{\Lambda}_P(t_{\text{inf}}, t_{\text{obs}})| \Big). \quad (2)$$

To assess the mismatches along each environmental axis $\vec{e}_i$, we can likewise define

$$\lambda_{C,i}(t_{\text{inf}}, t_{\text{obs}}) = \Omega\Big(|\vec{\Lambda}_C(t_{\text{inf}}, t_{\text{obs}}) \times \vec{e}_i|, |\tilde{\Lambda}_P(t_{\text{inf}}, t_{\text{obs}}) \times \vec{e}_i| \Big). \quad (3)$$

Within-region environmental filtering can be detected when $\delta_C(t_{\text{inf}}) < 0$. Communities composed of species whose overlapped climate niches are narrower than found under a regional expectation reflect the outcome of strong climate constraints. This is because fewer species with broad and variable climate tolerances can be found (e.g., climate generalists) compared to a random sample of the regional pool. Conversely, communities composed of species whose overlapped climate niches are broader than found under the null expectation ($\delta_C(t_{\text{inf}}) > 0$) may reflect the outcome of environmental permissiveness, because more climate space is occupied than expected. Alternatively $\delta_C(t_{\text{inf}}) > 0$ may instead indicate high microclimate variability that is not captured by a broadscale analysis.

Environmental disequilibrium can be detected when $\lambda_C(t_{\text{inf}},t_{\text{obs}}) > 0$. Communities with inferred climate at t_{inf} and observed climate at t_{obs} that are farther apart than expected contain species with niche centroids closer to other climates than those in the regional pool. Alternatively, communities with observed and inferred climates closer together than expected under the null expectation ($\lambda_C(t_{\text{inf}},t_{\text{obs}}) < 0$) indicate that more species with niche centroids close to the local climate have entered the community. Similar inferences hold when considering the mismatch along each climate axis.

Community climate deviations also can be mapped onto one or more of the three major processes in community assembly: environmental filtering, dispersal limitation, and species interactions (HilleRisLambers et al. 2012). Environmental filtering is directly reflected by $\delta_C(t_{\text{inf}})$, while dispersal limitation or species interactions can both be indicated by $\lambda_C(t_{\text{inf}},t_{\text{obs}})$. For example, positive values of $\lambda_C(t_{\text{inf}},t_{\text{obs}})$ could be caused by dispersal limitation relative to the regional pool or by species interactions leading to displacement of climatically more appropriate species. Negative values of $\lambda_C(t_{\text{inf}},t_{\text{obs}})$ could be caused by species interactions leading to increased niche packing, and thus, clustering of species' niches within climate space. The inability of $\lambda_C(t_{\text{inf}},t_{\text{obs}})$ to always distinguish these processes is similar to how either competition or environmental filtering can drive under-dispersion in phylogenetic (Swenson and Enquist 2009, Mayfield and Levine 2010, Bennett et al. 2013) and trait-based (Grime 2006) community ecology.

Climate mismatch deviations have several potential causes. These include lack of adaptive niche evolution, priority effects, limited propagule pressure, and competition, among others. Displacement of the community-inferred climate from the observed may be transient, indicating disequilibrium conditions due to inappropriate species persisting (trailing-edge lags) or appropriate species failing to colonize (leading-edge lags; see Dullinger et al. 2012, Svenning and Sandel 2013). On the other hand, the displacement may be maintained through time, perhaps because of stabilizing species interactions.

These statistics can be measured across time when sufficient data for observed climate or species composition are available. If observed climates are known at multiple times, then inferences of lag times can be made (Fig. 2A). If observed climate, community composition, and climate niches are known at multiple times, then

temporal variation in the strength of filtering and mismatch can be inferred (Fig. 2B).

Illustrating the Framework with New World Tree Communities

We demonstrate our community climate framework with data from the New World. Local community data come from 471 forest plots that are 0.1 ha in size spanning a 41° S to 53° N latitudinal range (Lamanna et al. 2014). These plots are measured using a standardized protocol (Gentry 1982) and represent a uniquely large sample of New World plant diversity. Mean per-plot richness is 69 ± 40 species (mean ± SD) species. Occurrence data come from more than a million observations of 14 697 woody species, and are aggregated over approximately the last 100 years. Regional species pools are variable across communities and are calculated for each as the set of species with at least one observation within the ecoregion containing the community (Olson et al. 2001). Mean pool richness is 2522 ± 1042 (mean ± SD) species.

Climate axes are defined as the annual minimum and maximum monthly temperature and precipitation. These axes are chosen for this demonstration analysis because of their broad importance for plant physiology. These axes are also somewhat correlated with each other, but we use them here primarily because of their conceptual simplicity. Climate data are obtained at three time points: averaged across the last forty years (present), within the Last Glacial Maximum (LGM), and within the Intergovernmental Panel on Climate Change's (IPCC) 2007 end-century A1B scenario (2080 CE). The LGM was chosen because it is representative for the late-Quaternary glacial–interglacial climate shifts, the strongest Quaternary climatic oscillations (Sandel et al. 2011), and the A1B scenario because of its relevance to contemporary global change. Full details of the data sources and analysis are found in *Materials and methods*.

In order to demonstrate how this framework can be used for hypothesis testing, we made a set of predictions. For the unscaled analysis, we expected that all communities would have nonzero climate mismatch relative to present-day climate, indicating disequilibrium between vegetation composition and contemporary climate. Spatially, we also expected that the climate mismatch would correlate negatively with absolute latitude (i.e., more mixing of species pools at the interface of North and South America) and the magnitude of climate change since the LGM (i.e., more change is harder to track), and that climate volume would correlate positively with species' mean range size (i.e., more generalists; see Morueta-Holme et al. 2013).

For the scaled analysis, we expected that all communities would show local-scale environmental filtering, and therefore negative climate volume deviations (HilleRisLambers et al. 2012). Similarly, we expected that communities would be in local-scale disequilibrium with past climate change and therefore show positive climate mismatch deviations (Svenning and Sandel 2013), though other community assembly processes may modulate this expectation. These predictions are consistent with empirical patterns of community assembly that we presented in the *Introduction*. We also predicted climate mismatch deviations would best reflect historical drivers, i.e., be minimized relative to LGM climate (Davis 1984) and maximized relative to rapidly shifting future climate (Bertrand et al. 2011). Spatially, we predicted that present-day climate volume deviations would be positively correlated with minimum annual temperature and precipitation because of the limiting effects of freezing and drought on plant physiology (Reyer et al. 2013). Finally, we predicted that present-day climate mismatch deviations would be positively correlated with the absolute magnitude of climate change since the LGM (i.e., changes in mean annual temperature and precipitation), because larger climate changes should be more challenging to track.

Materials and Methods

Mathematical definitions

Consider n climate axes that define a continuous real-valued environmental space $E \subset \Re^n$. A species S at time t has a realized climate niche $N_S(t) \subset E$ that can be inferred by transforming species observations in geographic space into climate space. Suppose also the community, C, has richness c.

We define the inferred climate of C at time t_{inf} as the mean median value of samples from the climate niche of each species i in the community averaged across r replicates.

$$\vec{E}_{\text{inf}}(t_{\text{inf}}) = \frac{1}{r}\sum_{j=1}^{r} Q\left(\bigcup_{i=1}^{c} \vec{\sigma}\left(N_i(t_{\text{inf}})\right), 0.5\right). \quad (4)$$

Here, $Q(x,y)$ is the yth quantile of x and $\vec{\sigma}(N)$denotes a single random sample from N.

We define community climate volume, $\Delta_C(t_{\text{inf}})$, through a proxy of the median distance to the inferred climate from random samples of each species' niche averaged across r replicates

$$\Delta_C(t_{\text{inf}}) = \frac{1}{r}\sum_{j=1}^{r} Q\left(\bigcup_{i=1}^{c} |\vec{\sigma}\left(N_{k_i}(t_{\text{inf}}) - \vec{E}_{\text{inf}}(t_{\text{inf}})\right)|, 0.5\right). \quad (5)$$

By sampling from each species' niche before making the median calculation, we effectively account for niche breadth. This distance-based metric is chosen because it is has fewer assumptions and is computationally much faster than other volume estimation methods (e.g., Cornwell et al. 2006; Blonder et al. 2014).

We also define community climate mismatch, $\vec{\Lambda}_C(t_{\text{inf}}, t_{\text{obs}})$, as the vector between the inferred climate at time t_{inf} and the observed climate at time t_{obs}

$$\vec{\Lambda}_C(t_{\text{inf}}, t_{\text{obs}}) = \vec{E}_{\text{inf}}(t_{\text{inf}}) - \vec{E}_{\text{obs}}(t_{\text{obs}}). \quad (6)$$

We define the rescaling function that transforms observed and null values of an arbitrary statistic A into a standardized effect size as

$$\Omega(A_{\text{obs}}, A_{\text{null}}) = \frac{A_{\text{obs}} - Q(A_{\text{null}}, 0.5)}{Q(A_{\text{null}}, 0.75) - Q(A_{\text{null}}, 0.25)}. \quad (7)$$

We finally define a two-tailed P value for this effect size

$$p(A_{\text{obs}}, A_{\text{null}}) = \text{If}\begin{cases} A_{\text{obs}} < \bar{A}_{\text{null}}, & \dfrac{2 \cdot |A_{\text{obs}} > A_{\text{null}}|}{|A_{\text{null}}|} \\ A_{\text{obs}} \geq \bar{A}_{\text{null}}, & \dfrac{2 \cdot |A_{\text{obs}} < A_{\text{null}}|}{|A_{\text{null}}|} \end{cases} \quad (8)$$

where vertical bars indicate the number of elements in each set.

Occurrence data

We obtained observations of plant occurrences through the BIEN database (Enquist et al. 2009), which integrates georeferenced plant observations from herbarium specimens, vegetation plot inventories, and species distributions maps for the New World (see footnote 13). All taxonomic names were standardized using the Taxonomic Name Resolution Service,[15] and all observations were geographically validated to ensure the accuracy of their reported locations. We retained noncultivated observations of only tree or liana species after assigning habit to each species from the TRY database (Kattge et al. 2011). We then retained only observations that were not part of the plot data described below, so that the occurrence and plot data would be independent from each other. The final dataset included 14 697 species and 1 083 361 observations. All these observations are assigned to $t_{\text{inf}} = t_{\text{pres}}$, but actually span approximately the last 100 years. We therefore make the assumption that the climate niche variation within this time period is much smaller than variation relative to t_{LGM} and t_{2080}.

Community data

We began by obtaining presence/absence data from a network of 575 0.1-ha Gentry-style forest plots (Gentry 1982). Every tree or liana individual in the plot with diameter at breast height greater than 2.5 cm was surveyed and was subsequently identified to species whenever possible. These plots have limited coverage in some important areas (e.g., Amazon basin, Pacific Northwest).

Because of the potential biases inherent in morphospecies identification and because of statistical requirements to have at least as many species as climate axes in each plot, we removed from the analysis all taxa that could not be identified to species level (morphospecies), resulting in a lower effective richness. We then retained plots (1) originally containing no more than 50% morphospecies, (2) having an effective richness of at least three, and (3) with an original richness less than the species pool richness. This process resulted in a final data set of 471 plots spanning a latitudinal range of 41° S to 53° N with mean richness of 69 ± 40 species (mean ± SD).

Climate data

We obtained climate data for four bioclimatic variables: maximum temperature of warmest month (10 × °C), minimum temperature of coolest month (10 × °C), precipitation of wettest month (mm), and precipitation of driest month (mm). We chose these four axes because they represent the extremes of two major axes of climate variation that are relevant to plants and are also easily interpreted. Data were obtained at 2.5-arcminute resolution for three different time periods. Present-day data came from the WorldClim data set (Hijmans et al. 2005). Last Glacial Maximum data (21 ky ago) was generated by the Community Climate System Model (CCSM; Braconnot et al. 2007). Future data for 2080 CE (Common Era) was generated by CCSM3 under the IPCC's 2007 SRES A1B scenario (*available online*).[16] Because of high skewness, we square-root-transformed the precipitation layers. We then transformed each layer $L_{i,t}$ (variable i, at time t) to a centered and scaled value relative to contemporary values as $L'_{i,t} = \Omega(L_{i,t}, L_{i,\text{pres}})$, after excluding Greenland from the analysis. Using this approach, the transformed climate variables represent standardized anomalies relative to present-day climate, and climate space distances can be compared between different time points.

Spatial predictors

We explored several potential predictors for community climate statistics. Minimum temperature and precipitation variables were obtained from present-day WorldClim data as BIO6 and BIO14, respectively. Climate shifts were calculated as the absolute value of the difference between present-day and Last Glacial Maximum mean annual temperature and precipitation. These shifts were calculated using the sources listed in *Materials and methods: Climate data*. Range size for species in each local community were calculated as convex hulls and obtained from the BIEN database (Morueta-Holme et al. 2013).

Implementation of framework

All analyses were conducted within the R statistical environment (R Development Core Team 2007) using our freely available "comclim" package. Climate niches for all species were obtained by transforming georefer-

[15] http://tnrs.iplantcollaborative.org

[16] http://bien.nceas.ucsb.edu

enced observations into climate space using present-day climate layers. Observed climate at each community was obtained by transforming the location of each community into climate space using present-day, past, or future layers.

Regional species pools were constructed by determining which species in the New World species pool had at least one occurrence into each of the World Wildlife Fund 299 New World global ecoregions (Olson et al. 2001). We then assigned each community to an ecoregion based on its location and defined its species pool as the set of species occurring within the ecoregion. Mean pool richness was 2522 ± 1042 species (mean ± SD). While other species pool definitions are possible and useful (Lessard et al. 2012*a*), we did not consider them for this study because our intent was primarily to demonstrate the framework in as simple a manner as possible.

Climate statistics were calculated for each community as the average of 100 random samples from the niche of each present species. To compute community climate deviations, we generated null communities for each community. Community compositions reflected random sampling (with replacement) from the regional species pool preserving the species richness of the observed community. We generated 100 null communities and then followed the procedure for the observed communities to generate the distributions $\tilde{\Delta}_P$ and $\tilde{\Lambda}_P$. We then used these distributions to calculate δ_C and λ_C.

Results

We created community climate diagrams for all 471 communities. An example is shown in Fig. 3.

Unscaled analysis

We found strong spatial gradients in community climate statistics (Fig. 4). Community climate volume ($\Delta_C(t_{\text{inf}})$) was largest in the tropics (Pearson's $\rho = -0.48$, $P < 10^{-16}$) and was correlated with mean range size as expected ($\rho = 0.42$, $P < 10^{-16}$). Contrary to expectation, community climate mismatch ($|\vec{\Lambda}(t_{\text{pres}}, t_{\text{pres}})|$) did not show a latitudinal gradient ($P = 0.09$). However, larger mismatch values were found at sites with higher minimum precipitation ($\rho = 0.56$, $P < 10^{-16}$) or higher changes in precipitation since the LGM ($\rho = 0.54$, $P < 0.01$), the latter indicating some control of contemporary species composition by paleoclimate. Both volume and mismatch were also correlated with species pool richness and local richness.

Scaled analysis

We found that 435 out of 471 communities showed $\delta_C(t_{\text{pres}}) < 0$, consistent with strong environmental filtering from the regional pool, and $\lambda_C(t_{\text{pres}},t_{\text{pres}}) > 0$ for 112 out of 471 communities, consistent with local environmental equilibrium in the majority of communities (Fig. 5). Some climate axes showed more disequilibrium than others (Fig. 6). The mean value of $\lambda_{C,i}(t_{\text{pres}}, t_{\text{pres}})$ was negative for maximum and minimum temperature (−1.3 and −0.6, respectively) and positive for maximum and minimum precipitation (0.2 and 0.5, respectively).

We next determined at what times climate mismatches were minimized. We found that $\lambda_C(t_{\text{pres}},t_{\text{LGM}}) < \lambda_C(t_{\text{pres}},t_{\text{pres}})$ for about one-half of all communities (244/471; $\chi^2_1 = 0.61$, $P = 0.43$), indicating statistically indistinguishable levels of equilibrium between present-day vegetation and LGM climate and present-day vegetation and present climate. However, we did find that $\lambda_C(t_{\text{pres}},t_{\text{pres}}) < \lambda_C(t_{\text{pres}},t_{2080})$ for most communities (283/471; $\chi^2_1 = 21.46$, $P < 10^{-5}$). These results indicate that most communities will come into greater disequilibrium with near-future climate change, i.e., in the absence of species turnover or range shifts.

Spatial predictors of community climate deviations showed a weak latitudinal gradient (Fig. 7). Climate volume deviations ($\delta_C(t_{\text{pres}})$) were larger when minimum precipitation ($\rho = 0.42$, $P < 10^{-16}$) or mean range size ($\rho = 0.26$, $P < 10^{-8}$) were higher, consistent with predictions. Volume deviations were also higher in sites with more temperature ($\rho = 0.21$, $P < 10^{-5}$) and precipitation ($\rho = 0.27$, $P < 10^{-8}$) change since the LGM, indicating that climatically unstable areas have local communities more structured by environmental filtering. Climate mismatch deviations ($\lambda_C(t_{\text{pres}},t_{\text{pres}})$) were larger at sites with larger-ranged species ($\rho = 0.50$, $P < 10^{-16}$), consistent with predictions, and also larger for more temperature change since the LGM ($\rho = 0.40$, $P < 10^{-16}$). There were only limited effects on either statistic of regional pool or local richness.

Discussion

Interpretation of empirical results

Our finding of mismatch between community composition and contemporary climate runs contrary to a key assumption of climate proxies based on species composition data. These use occurrence data from paleo-communities (e.g., pollen cores, packrat middens, or insect fragments; see Birks et al. 2010) to infer climate based on overlapping species' climate niches (Kühl et al. 2002) and assume that $\vec{\Lambda}(t_{\text{inf}}, t_{\text{obs}}) = 0$. In the forest plots analyzed, we found that values of $|\vec{\Lambda}(t_{\text{pres}}, t_{\text{pres}})|$ took a mean value of 0.41 ± 0.32 (mean ± SD), a distribution that is significantly different than zero ($P < 10^{-16}$) and consistent with one-dimensional studies of climate mismatch (Clavero et al. 2011, Devictor et al. 2012). This result indicates that better understandings of the drivers of mismatch are needed before these paleoclimate proxies can be confidently applied.

Our scaled analysis showed that most forest communities show environmental filtering and environmental equilibrium relative to their regional species pools, while a smaller number are also in climatic disequilibrium at this spatial scale. The finding of strong environmental filtering is consistent with the results of many trait-based and phylogeny-based studies (HilleRisLambers et al.

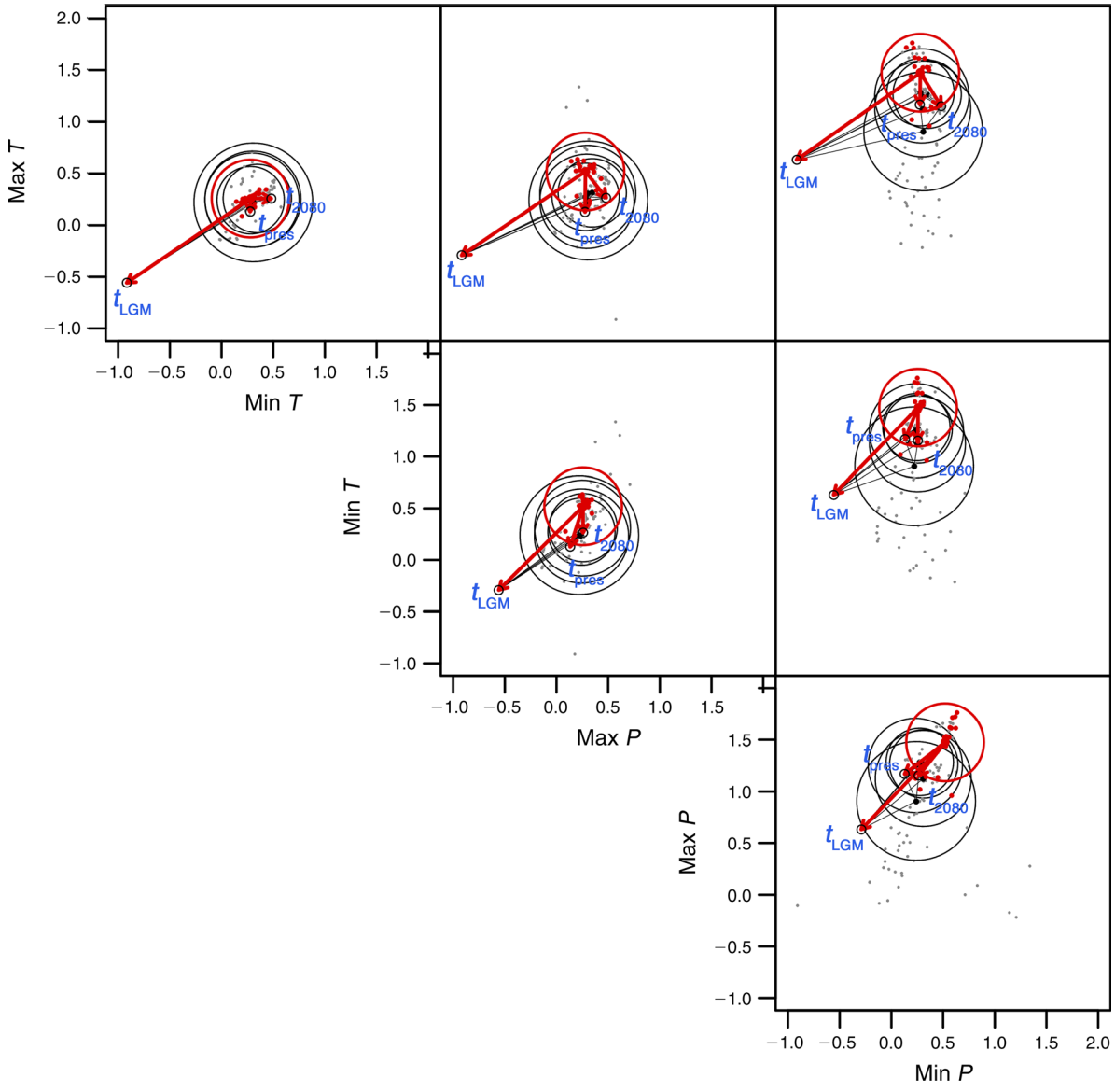

FIG. 3. Example community climate diagram for the CARY forest plot at the Institute of Ecosystem Studies in Dutchess County, New York, USA. Each panel shows a two-dimensional projection of the rescaled climate space. The solid red dot indicates the inferred climate of the community, while individual red dots indicate centroids of species' niches. The climate volume at $t_{inf} = t_{pres}$ is drawn as a red-outlined circle, and the climate mismatch is drawn from the inferred climate at $t_{inf} = t_{pres}$ to three observed climates: contemporary ($t_{obs} = t_{pres}$), future A1B scenario in the year 2080 CE ($t_{obs} = t_{2080}$), and Last Glacial Maximum (LGM) ($t_{obs} = t_{LGM}$). Five null communities sampled from the regional species pool are shown with species' centroids as gray points and climate volumes as black circles. Via scaled statistics, this community shows filtering ($\delta_C(t_{pres}) = -0.3$; red circle smaller than black circles) and disequilibrium ($\lambda_C(t_{pres}, t_{pres}) = 5.4$; red vectors longer than thin black vectors for the $t_{obs} = t_{pres}$ climate). Via unscaled statistics, this community also shows an absolute climate volume ($\Delta_C(t_{pres}) = 0.4$) and climate mismatch ($|\vec{\Lambda}(t_{pres}, t_{pres})| = 0.5$) that are both smaller than across other communities shown in Fig. 4. Abbreviations are: pres, present; *T*, temperature; *P*, precipitation; min, minimum; and max, maximum.

2012). The scarcity of forest communities showing local-scale environmental disequilibrium relative to their regional species pools indicates that local communities' composition are no more mismatched to climate than their regional pools are, consistent with an absence of additional local-scale assembly processes. This result may be influenced by our particular choice of species pool, which was chosen primarily for conceptual clarity, or the 100-year temporal aggregation of occurrence data for $t_{inf} = t_{pres}$. Where we do find disequilibrium, it is primarily linked to precipitation: our axis-by-axis analysis showed that contemporary plant communities closely track temperature, but show the most mismatched response to precipitation. This precipitation

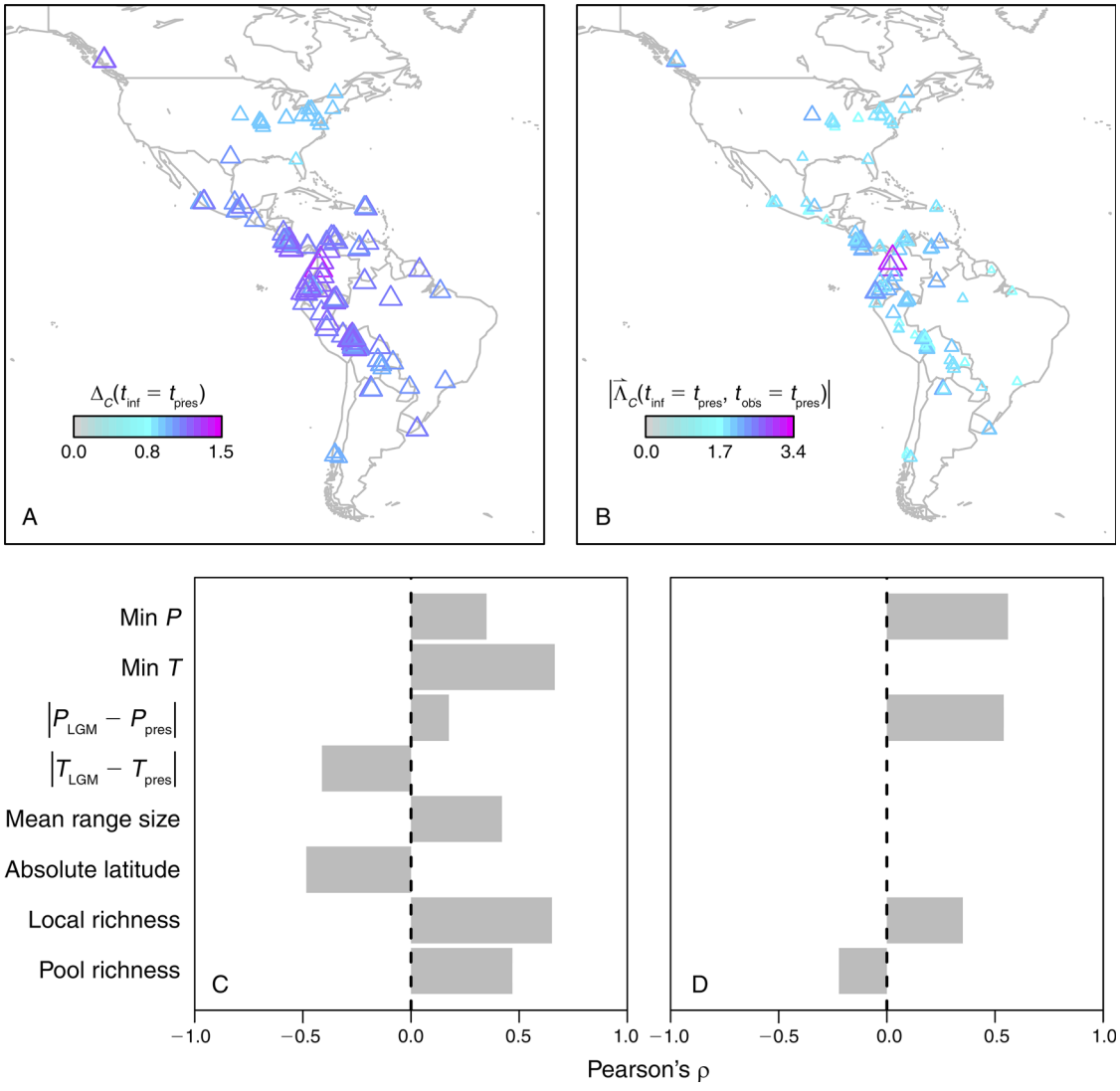

FIG. 4. Unscaled results: Spatial patterns and predictors of (A) $\Delta_C(t_{pres})$ (climate volume) and (B) $|\vec{\Lambda}_C(t_{pres}, t_{pres})|$ (climate mismatch). Communities are colored and sized by their magnitude. The statistics are associated with a range of spatially variable predictors, shown in panel (C) for $\Delta_C(t_{pres})$ and panel (D) for $|\vec{\Lambda}_C(t_{pres}, t_{pres})|$. Histogram bar lengths indicate the Pearson correlation coefficient between each predictor and community climate statistic and are not shown if the correlation is not significant at the $\alpha = 0.05$ level. Abbreviations are: pres, present; T, temperature; P, precipitation; and min, minimum.

mismatch deviation contrasts with an earlier study of temperature lag in herbaceous-only species (Bertrand et al. 2011) but is consistent with the correlation of paleoprecipitation change with climate deviations seen across communities in this analysis.

Our spatial analysis indicated that environmental filtering and disequilibrium are partially predictable from site characteristics. Correlations in both deviations were associated with the magnitude of climate change since the LGM, indicating that community composition is still responding to past climate change. Note however that LGM climate estimates remain poorly constrained between different models, so this result should be viewed as preliminary. Nevertheless, our analysis does suggest that current and future climate change will further move these communities even farther from climatic equilibrium.

Limitations of the framework

Our community climate framework comes with three important limitations. First, inferences from the scaled version of the framework are sensitive to the definition of the regional species pool and other attributes of the null model. Of most importance, the definition of the species pool affects the deviation of estimates and statistical power (Gotelli and Graves 1996, Gotelli and Ulrich 2012), both of which can lead to misinterpretation of the biological meaning of the results (Swenson et

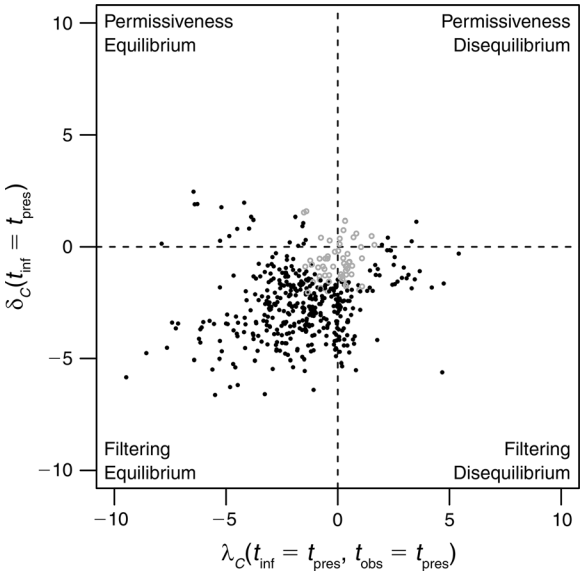

FIG. 5. Distribution of community climate deviations across 471 New World tree communities. Each point represents a unique 0.1-ha plot. The differing interpretations of the statistics are shown in each corner. Plots for which at least one statistic is significantly different from zero are shown as black dots; otherwise as gray circles.

al. 2006, Lessard et al. 2012*b*). The geographic extent and configuration of each community's regional pool may affect our results. For example, the ecoregional pools we used are already environmentally filtered from the global species pool, making inferences of local-scale filtering more powerful; on the other hand, a larger regional pool may be more appropriate for assessing disequilibrium due to postglacial recolonization. Additionally, the null model used in the demonstration analysis does not incorporate abundance or demographic information (e.g., as in Gotelli et al. 2010). Rare and common species are given equal weight when computing community climate statistics, which may especially bias disequilibrium inferences. The comclim R package does allow for weighted sampling and variable definitions of species pools for each community. We suggest that real-world analyses examine the sensitivity of results to several species pool definitions (Lessard et al. 2012*b*).

Second, the approach assumes that the realized climate niche is a good representation of the fundamental climate niche defined by physiological tolerances (e.g., Araújo et al. 2013). Bias in community climate deviations would occur if fundamental niches were systematically displaced in one direction relative to realized niches (e.g., because of modulation by land use; Clavero et al. 2011). Conceptual arguments (Peterson et al. 2011) and empirical data from a range of taxa (Araújo et al. 2013) have shown that systematic rather than random displacement can occur, with fundamental niches often extending into regions of climate space not currently filled by a species or with contemporary abundance peaking in regions of climate space far from the physiological optimum (Murphy et al. 2006). This is an unavoidable limitation of observational data. Our framework can be modified to use fundamental climate niche data by replacing the mapping from occurrence data to climate space with a response surface determined via experiment (Colwell and Fuentes 1975). Such data are now becoming available along a limited set of climate axes for some animals (Kearney and Porter 2004) and some plants (Araújo et al. 2013). Regardless, our finding of local climatic equilibrium relative to regional species pools, contrary to expectation, may partially be driven by an inability to capture the fundamental niche of each species.

Third, the use of differing climate axes can also modulate inferences, because species' niches may appear very different when projected in different climate dimensions. This issue is also relevant to species distribution modeling (Peterson et al. 2011), and we recommend similar guidelines for axis choice: as small a number as possible and as physiologically relevant as possible. If these issues are concerning, it is also possible to repeat analyses for various combinations of climate axes or species pool definitions, e.g., via ensemble modeling (Araújo and New 2007).

Future opportunities

Climate shows variability at multiple timescales (e.g., decadal, millennial, interglacial), with species responding differently at each scale depending on factors such as adaptive potential, lifespan, and dispersal ability (Davis 1984). Our framework provides an approach to quantify these dynamics of disturbance, succession, and paleoclimate change. The necessary data are climate and occurrence data for multiple time points. This approach

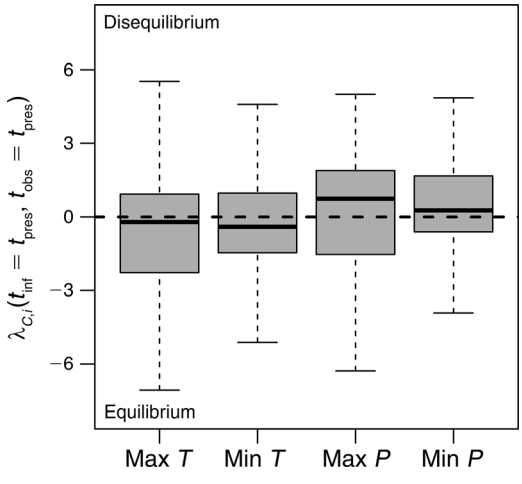

FIG. 6. Vector components of community climate mismatch deviations, indicating which axes of climate are in disequilibrium with species composition. Distributions are calculated across communities. Axes are maximum temperature (max T), minimum temperature (min T), maximum precipitation (max P), and minimum precipitation (min P).

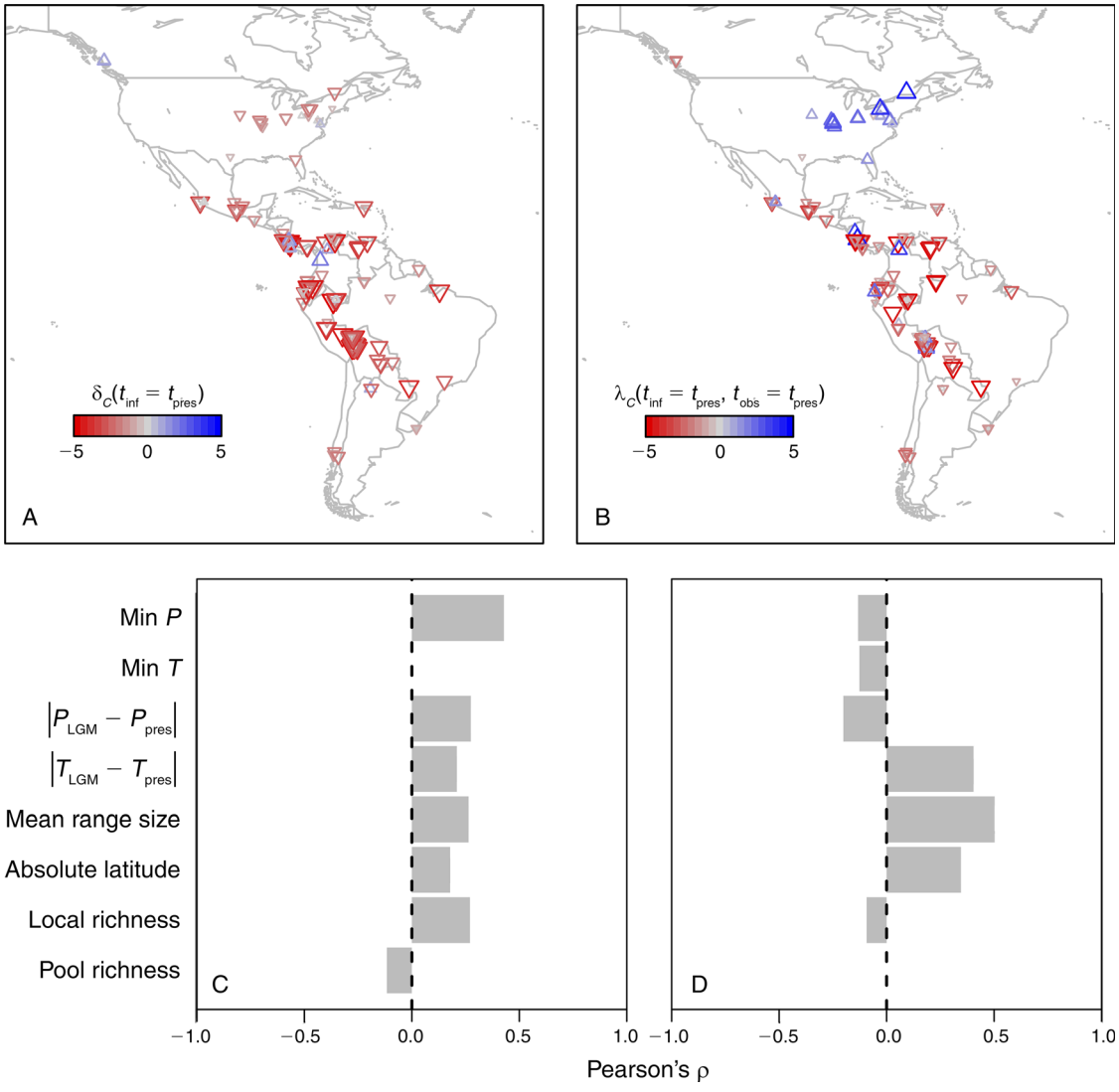

FIG. 7. Scaled results: Spatial patterns and predictors of (A) $\delta_C(t_{pres})$ (climate volume) and (B) $\lambda_C(t_{pres},t_{pres})$ (climate mismatch). Communities are colored and sized by their magnitude and drawn with upward triangle if positive and downward triangle if negative. The statistics are associated with a range of spatially variable predictors, shown in panel (C) for $\delta_C(t_{pres})$ and panel (D) for $\lambda_C(t_{pres},t_{pres})$. Histogram bar lengths indicate the Pearson correlation coefficient between each predictor and community climate statistic, and are not shown if the correlation is not significant at the $\alpha = 0.05$ level.

is especially important when climate-niche evolution, niche shifts, or variation in community and species pool composition occur over time (Broennimann et al. 2011, Blois et al. 2012, Petitpierre et al. 2012). For example, community climate mismatches can be calculated from the present day relative to a range of past climates if paleoclimate data are available. Recent advances with global circulation models (Collins et al. 2006) are enabling better reconstruction of paleoclimate at more time points than those studied here (i.e., just the LGM). If paleo-niche data are also available, then it also becomes possible to assess community climate mismatches and volumes at an arbitrary time in the past. Such data can be obtained through several routes: if occurrence data are also available at multiple times, they can be combined with paleoclimate layers; alternatively climate niches can be reconstructed directly using phylogenetic approaches (Lavergne et al. 2013).

Our New World analysis is intended primarily as a demonstration, but our community climate framework can be applied widely. One advantage of the framework is the ability to recast assembly processes in terms of lagged selection on climate niches, providing a novel temporal perspective that complements phylogenetic and trait-based frameworks. A second advantage is easily satisfied data requirements. Data that will allow application to a wider range of taxa and spatial scales are becoming increasingly available. Initiatives like

BIEN are being developed for plant distributions and assemblage composition in China (Fang et al. 2012) and Europe (Dengler et al. 2011). Similar initiatives also exist for mammals (Thibault et al. 2011) and birds (e.g., Breeding Bird Survey; *available online*).[17] Moreover, paleo-assemblage and paleo-occurrence data are also becoming more available through recent database efforts (e.g., Neotoma; *available online*).[18] Paired with the growing availability of high-quality, spatially resolved paleoclimate estimates from general circulation models (e.g., Liu et al. 2009) and climate niche reconstructions based on phylogeny (Evans et al. 2009), reconstructing climate niches of multiple species and communities should soon become achievable (Nogués-Bravo 2009).

Acknowledgments

We thank Robert Colwell for his thoughtful comments. This work was conducted as part of the Botanical Information Ecology Network (BIEN) working group, supported by the National Center for Ecological Analysis and Synthesis (NSF grant #EF-0553768), the University of California Santa Barbara, and the state of California. The BIEN working group was also supported by iPlant (NSF grant #DBI-0735191). We thank many collaborators for sharing data with BIEN. A full list of data providers is available at http://bien.nceas.ucsb.edu/bien/people/data-contributors/. B. Blonder was supported by a NSF predoctoral fellowship and a Nordic Research Opportunity award cosponsored through the Danish National Research Foundation's Center for Macroecology, Evolution and Climate. M. K. Borregaard and D. Nogués-Bravo are supported by a Sapere Aude grant from the Danish Council for Independent Research (Natural Sciences). J. C. Donoghue was supported by the iPlant Collaborative. P. M. Jørgensen was supported by the National Science Foundation (DEB-0743457). J.-P. Lessard was supported by the Quebec Centre for Biodiversity Science Postdoctoral Fellowship. N. Morueta-Holme acknowledges support from an EliteForsk Award and the Aarhus University Research Foundation. D. Nogués-Bravo and C. Rahbek thank the Danish National Research Foundation for its support of the Center for Macroecology, Evolution and Climate. J.-C. Svenning was supported by the European Research Council (ERC-2012-StG-310886-HISTFUNC). B. J. Enquist was supported by an NSF Macrosystems grant (EF-1065844) and a fellowship from the Aspen Center for Environmental Studies.

Literature Cited

Araújo, M. B., F. Ferri-Yáñez, F. Bozinovic, P. A. Marquet, F. Valladares, and S. L. Chown. 2013. Heat freezes niche evolution. Ecology Letters 16:1206–1219.

Araújo, M. B., and M. New. 2007. Ensemble forecasting of species distributions. Trends in Ecology and Evolution 22: 42–47.

Bennett, J. A., E. G. Lamb, J. C. Hall, W. M. Cardinal-McTeague, and J. F. Cahill. 2013. Increased competition does not lead to increased phylogenetic overdispersion in a native grassland. Ecology Letters 16:1168–1176.

Bertrand, R., J. Lenoir, C. Piedallu, G. Riofrio-Dillon, P. de Ruffray, C. Vidal, J.-C. Pierrat, and J.-C. Gegout. 2011. Changes in plant community composition lag behind climate warming in lowland forests. Nature 479:517–520.

Birks, H., O. Heiri, H. Seppä, and A. E. Bjune. 2010. Strengths and weaknesses of quantitative climate reconstructions based on late-Quaternary biological proxies. Open Ecology Journal 3:68–110.

Birks, H. J. B. 1998. Numerical tools in palaeolimnology: progress, potentialities, and problems. Journal of Paleolimnology 20:307–332.

Blois, J. L., J. W. Williams, M. C. Fitzpatrick, S. Ferrier, S. D. Veloz, F. He, Z. Liu, G. Manion, and B. Otto-Bliesner. 2012. Modeling the climatic drivers of spatial patterns in vegetation composition since the Last Glacial Maximum. Ecography 36: 460–473.

Blonder, B., C. Lamanna, C. Violle, and B. J. Enquist. 2014. The *n*-dimensional hypervolume. Global Ecology and Biogeography 23:595–609.

Braconnot, P., et al. 2007. Results of PMIP2 coupled simulations of the Mid-Holocene and Last Glacial Maximum. Part 1: experiments and large-scale features. Climate of the Past 3(2):261–277.

Broennimann, O., et al. 2011. Measuring ecological niche overlap from occurrence and spatial environmental data. Global Ecology and Biogeography 21:481–497.

Clavero, M., D. Villero, and L. Brotons. 2011. Climate change or land use dynamics: do we know what climate change indicators indicate? PLoS ONE 6:e18581.

Collins, W. D., C. M. Bitz, M. L. Blackmon, G. B. Bonan, C. S. Bretherton, J. A. Carton, P. Chang, S. C. Doney, J. J. Hack, and T. B. Henderson. 2006. The community climate system model version 3 (CCSM3). Journal of Climate 19:2122–2143.

Colwell, R. K., and E. R. Fuentes. 1975. Experimental studies of the niche. Annual Review of Ecology and Systematics 6: 281–310.

Cornwell, W. K., D. W. Schwilk, and D. D. Ackerly. 2006. A trait-based test for habitat filtering: convex hull volume. Ecology 87:1465–1471.

Davis, M. B. 1984. Climatic instability, time, lags, and community disequilibrium. Pages 269–284 *in* J. Diamond and T. Case, editors. Community ecology. Harper and Row, New York, New York, USA.

Dengler, J., F. Jansen, F. Glöckler, R. K. Peet, M. De Cáceres, M. Chytry, J. Ewald, J. Oldeland, G. Lopez-Gonzalez, and M. Finckh. 2011. The global index of vegetation plot databases (GIVD): a new resource for vegetation science. Journal of Vegetation Science 22:582–597.

Devictor, V., et al. 2012. Differences in the climatic debts of birds and butterflies at a continental scale. Nature Climate Change 2:121–124.

Dullinger, S., et al. 2012. Extinction debt of high-mountain plants under twenty-first-century climate change. Nature Climate Change 2:619–622.

Enquist, B. J., R. Condit, R. K. Peet, M. Schildhauer, and B. Thiers. 2009. The botanical information and ecology network (BIEN): cyberinfrastructure for an integrated botanical information network to investigate the ecological impacts of global climate change on plant biodiversity. The iPlant Collaborative, Tuscon, Arizona, USA. www.iplantcollaborative.org/sites/default/files/BIEN_White_Paper.pdf

Evans, M. E. K., S. A. Smith, R. S. Flynn, and M. J. Donoghue. 2009. Climate, niche evolution, and diversification of the "bird-cage" evening primroses (*Oenothera*, sections *Anogra* and *Kleinia*). American Naturalist 173:225–240.

Fang, J., Z. Shen, Z. Tang, X. Wang, Z. Wang, J. Feng, Y. Liu, X. Qiao, X. Wu, and C. Zheng. 2012. Forest community survey and the structural characteristics of forests in China. Ecography 35:1059–1071.

Gentry, A. 1982. Patterns of Neotropical plant species diversity. Evolutionary Biology 15:1–84.

Gotelli, N. J., and G. R. Graves. 1996. Null models in ecology. Smithsonian Institution Press, Washington, D.C., USA.

[17] https://www.pwrc.usgs.gov/bbs/RawData/

[18] http://www.neotomadb.org/data

Gotelli, N. J., G. R. Graves, and C. Rahbek. 2010. Macroecological signals of species interactions in the Danish avifauna. Proceedings of the National Academy of Sciences USA 107:5030–5035.

Gotelli, N. J., and W. Ulrich. 2012. Statistical challenges in null model analysis. Oikos 121:171–180.

Grime, J. P. 2006. Trait convergence and trait divergence in herbaceous plant communities: mechanisms and consequences. Journal of Vegetation Science 17:255–260.

Hawkins, B. A., M. Rueda, T. F. Rangel, R. Field, and J. A. F. Diniz-Filho. 2014. Community phylogenetics at the biogeographical scale: cold tolerance, niche conservatism and the structure of North American forests. Journal of Biogeography 41:23–38.

Hijmans, R., S. Cameron, J. Parra, P. Jones, and A. Jarvis. 2005. Very high resolution interpolated climate surfaces for global land areas. International Journal of Climatology 25: 1965–1978.

HilleRisLambers, J., P. B. Adler, W. S. Harpole, J. M. Levine, and M. M. Mayfield. 2012. Rethinking community assembly through the lens of coexistence theory. Annual Review of Ecology, Evolution, and Systematics 43:227–248.

Kattge, J., et al. 2011. TRY—a global database of plant traits. Global Change Biology 17:2905–2935.

Kearney, M., and W. P. Porter. 2004. Mapping the fundamental niche: physiology, climate, and the distribution of a nocturnal lizard. Ecology 85:3119–3131.

Kraft, N. J., R. Valencia, and D. D. Ackerly. 2008. Functional traits and niche-based tree community assembly in an Amazonian forest. Science 322:580–582.

Kühl, N., C. Gebhardt, T. Litt, and A. Hense. 2002. Probability density functions as botanical-climatological transfer functions for climate reconstruction. Quaternary Research 58: 381–392.

La Sorte, F. A., and W. Jetz. 2012. Tracking of climatic niche boundaries under recent climate change. Journal of Animal Ecology 81:914–925.

Lamanna, C. A., et al. 2014. Functional trait space and the latitudinal diversity gradient. Proceedings of the National Academy of Sciences USA 111:13745–13750.

Lavergne, S., M. Evans, I. Burfield, F. Jiguet, and W. Thuiller. 2013. Are species' responses to global change predicted by past niche evolution? Philosophical Transactions of the Royal Society of London B 368:1610.

Lenoir, J., et al. 2013. Local temperatures inferred from plant communities suggest strong spatial buffering of climate warming across Northern Europe. Global Change Biology 19:1470–1481.

Lessard, J. P., J. Belmaker, J. A. Myers, J. M. Chase, and C. Rahbek. 2012*b*. Inferring local ecological processes amid species pool influences. Trends in Ecology and Evolution 27: 600–607.

Lessard, J.-P., M. K. Borregaard, J. A. Fordyce, C. Rahbek, M. D. Weiser, R. R. Dunn, and N. J. Sanders. 2012*a*. Strong influence of regional species pools on continent-wide structuring of local communities. Philosophical Transactions of the Royal Society of London B 279:266–274.

Liu, Z., B. Otto-Bliesner, F. He, E. Brady, R. Tomas, P. Clark, A. Carlson, J. Lynch-Stieglitz, W. Curry, and E. Brook. 2009. Transient simulation of last deglaciation with a new mechanism for Bølling-Allerød warming. Science 325:310–314.

Mayfield, M. M., and J. M. Levine. 2010. Opposing effects of competitive exclusion on the phylogenetic structure of communities. Ecology Letters 13:1085–1093.

Morueta-Holme, N., et al. 2013. Habitat area and climate stability determine geographical variation in plant species range sizes. Ecology Letters 16:1446–1454.

Mosbrugger, V., T. Utescher, and D. L. Dilcher. 2005. Cenozoic continental climatic evolution of Central Europe. Proceedings of the National Academy of Sciences USA 102: 14964.

Murphy, H. T., J. VanDerWal, and J. Lovett-Doust. 2006. Distribution of abundance across the range in eastern North American trees. Global Ecology Biogeography 15:63–71.

Nogués-Bravo, D. 2009. Predicting the past distribution of species climatic niches. Global Ecology Biogeography 18: 521–531.

Olson, D. M., E. Dinerstein, E. D. Wikramanayake, N. D. Burgess, G. V. N. Powell, E. C. Underwood, J. A. D'Amico, I. Itoua, H. E. Strand, and J. C. Morrison. 2001. Terrestrial ecoregions of the world: a new map of life on Earth. A new global map of terrestrial ecoregions provides an innovative tool for conserving biodiversity. BioScience 51:933–938.

Ordonez, A. 2013. Realized climate niche of North American plant taxa lagged behind climate during the end of the Pleistocene. American Journal of Botany 100:1255–1265.

Peterson, A. T., J. Soberon, R. G. Pearson, R. P. Anderson, E. Martinez-Meyer, M. Nakamura, and M. B. Araujo. 2011. Ecological niches and geographic distributions (MPB-49). Princeton University Press, Princeton, New Jersey, USA.

Petitpierre, B., C. Kueffer, O. Broennimann, C. Randin, C. Daehler, and A. Guisan. 2012. Climatic niche shifts are rare among terrestrial plant invaders. Science 335:1344–1348.

Pottier, J., A. Dubuis, L. Pellissier, L. Maiorano, L. Rossier, C. F. Randin, P. Vittoz, and A. Guisan. 2012. The accuracy of plant assemblage prediction from species distribution models varies along environmental gradients. Global Ecology Biogeography 22:52–63.

R Development Core Team. 2007. R: a language and environment for statistical computing. R Foundation for Statistical Computing, Vienna, Austria. www.r-project.org

Reyer, C. P. O., et al. 2013. A plant's perspective of extremes: terrestrial plant responses to changing climatic variability. Global Change Biology 19:75–89.

Sandel, B., L. Arge, B. Dalsgaard, R. Davies, K. Gaston, W. Sutherland, and J.-C. Svenning. 2011. The influence of Late Quaternary climate-change velocity on species endemism. Science 334:660–664.

Svenning, J. C., and B. Sandel. 2013. Disequilibrium vegetation dynamics under future climate change. American Journal of Botany 100:1266–1286.

Swenson, N. G., and B. J. Enquist. 2007. Ecological and evolutionary determinants of a key plant functional trait: wood density and its community-wide variation across latitude and elevation. American Journal of Botany 94: 451–459.

Swenson, N. G., and B. J. Enquist. 2009. Opposing assembly mechanisms in a Neotropical dry forest: implications for phylogenetic and functional community ecology. Ecology 90: 2161–2170.

Swenson, N. G., B. J. Enquist, J. Pither, J. Thompson, and J. K. Zimmerman. 2006. The problem and promise of scale dependency in community phylogenetics. Ecology 87:2418–2424.

Thibault, K. M., S. R. Supp, M. Giffin, E. P. White, and S. M. Ernest. 2011. Species composition and abundance of mammalian communities. Ecology 92:2316.

Webb, C. O., D. D. Ackerly, M. A. McPeek, and M. J. Donoghue. 2002. Phylogenies and community ecology. Annual Review of Ecology, Evolution, and Systematics 33: 475–505.